Journal of Physics: Conference Series

Application of Time Synchronous Averaging in Mitigating UAV Noise and Signal Loss for Continuous Scanning Laser Doppler Vibrometry

Application of Time Synchronous Averaging in Mitigating UAV Noise and Signal Loss for Continuous Scanning Laser Doppler Vibrometry

M Mohammadi[1*], S Oberst[2] & B J Halkon[1,2]

[1]School of Mechanical and Mechatronic Engineering,
[2]Centre for Audio, Acoustics and Vibration,
Faculty of Engineering and Information Technology,
University of Technology Sydney, Ultimo, NSW 2007, Australia

[*]Mahdi.Mohammadi@student.uts.edu.au

Abstract: The laser Doppler vibrometer (LDV) has been shown to be effective for a wide application of vibration assessments that are well accepted. One of the new avenues for exploring alternative measurement scenarios, mounting LDVs on unmanned aerial vehicles (UAVs) is emerging as a potential avenue for remote and harsh environment measurements. Such configurations grapple with the challenge of the LDV sensor head being sensitive to UAV vibration during flight and signal loss due to tracking error. This study investigates the effectiveness of several Time Synchronous Averaging (TSA) techniques to circumvent these obstacles. Through comprehensive evaluations, all three TSA techniques under investigation demonstrated significant potential in suppressing UAV-induced noise and minimising the effects of signal dropout. Traditional TSA showcased a remarkable sixfold enhancement in signal quality when analysed via the mean square error. However, the study also highlighted that while TSA and Multi-Cycle Time Synchronous Average (MCTSA) elevated signal clarity, there is a trade-off between noise suppression and signal duration. Additionally, the findings emphasise the importance of synchronisation between scanning and target vibration. To achieve optimal results in Continuous Scanning Laser Doppler Vibrometer measurements, there is a need for advanced algorithms capable of estimating target vibration and synchronising scanning in real-time. As the study was rooted in steady-state vibrations, future research should explore transient vibration scenarios, thereby broadening the application scope of TSA techniques in UAV-mounted LDV systems.

1. Introduction

Engineers tasked with the maintenance of machines, structures, vehicles or instruments use vibrations to characterize the health of a system during its operation. This occurs because all objects, whether moving or stationary, emit low levels of vibration caused by internal excitation or external, environmental factors [1]. Conventionally, accelerometers have been the go-to instrument for measuring vibrations. However, in scenarios where accelerometers are unsuitable—be it due to environmental conditions or system constraints—a more advanced technology emerges as a viable alternative: the laser Doppler vibrometer (LDV) [2]. The basic operating principle of an LDV system relies on a two-beam laser interferometer that measures the frequency shift between an internal reference beam and a test beam. The test beam is aimed towards the surface of interest and the scattered light from the target

surface is collected by the sensor head and combined with the reference beam. By comparing the frequency shift between the two beams using an interferometer, LDVs can remotely discern even the minutest of vibrations [3].

Building on the foundational principles of the LDV, Continuous-scan Laser Doppler Vibrometry (CSLDV) was developed as a further innovation. Unlike its predecessor which concentrates its beam on one point during measurements, CSLDV sweeps its laser continuously across the surface, enabling the capture of motion across multiple points simultaneously [4]. This continuous scanning feature of the CSLDV presents a distinct advantage, especially when dealing with expansive structures such as bridges or large buildings which would traditionally require multiple sensors. Research spearheaded by figures like Allen & Sracic has emphasized how CSLDV can obtain high-resolution structural mode shapes in a fraction of the time compared with traditional LDV systems [5].

Simultaneously, Unmanned Aerial Vehicles (UAVs) have seen widespread adoption across various sectors due to their numerous applications, operational flexibility, and potential for cost-effectiveness. Specifically, within the realm of infrastructure and structural health monitoring, UAVs mounted with a variety of sensors and imaging devices have emerged as tool for remote, non-destructive evaluation that can be safely controlled by a human operator[6]. This shift in assessment techniques overcomes several challenges inherent to traditional methods such as accessibility, safety concerns, time constraints and cost inefficiencies. The mobility and agility of UAVs further empower them to swiftly inspect vast infrastructures or multiple structures within a limited timeframe. Recent research has showcased a variety of unique frameworks from full field mapping of entire bridges using image processing systems for crack detection [7] to structural assessments of large wind turbines using target free Discriminative Scale Space Tracker (DSST) vision algorithms [8]. These applications of UAV-borne sensors highlight the potential for cost-effective and efficient structural monitoring of expansive civil infrastructures.

Given the immense potential and benefits of UAVs in structural monitoring, there is an increasing need for UAV mounted LDV solutions. But while UAVs equipped with LDV's introduce unprecedented capabilities, they come with a unique set of problems that are not present with other sensors [2]. The most significant of these factors being the vibration of the LDV's sensor head. When LDVs are mounted on vibrating platforms, the vibration of the surface is transferred to the LDV sensor head. This produces an interference pattern that is subsequently transferred to the measurement signal [9]. It becomes impossible to distinguish between the vibration of the sensor head and that of the target being measured as the LDV only detects a doppler shift in the light – it cannot isolate the cause of the shift. To mitigate this challenge, researchers have proposed techniques such as employing accelerometer(s) behind the instrument sensor head that can be used as a reference signal to extract the vibration of the sensor head from the LDV signal [10]. Such methodologies, coupled with other time domain post-processing-based approaches, can substantially enhance the accuracy of LDV measurements, especially in high-vibration scenarios such as those encountered with UAVs.

Another challenge in LDV-mounted UAV solutions arises from the necessity of a tracking system to precisely target specific points on a structure for vibration measurement[12]. Even minor misalignments can lead to signal loss or flawed data, a critical concern when the UAV is subjected to dynamic environmental factors such as wind or turbulence[13]. Acknowledging that there will always be some level of tracking error is inevitable in these complex conditions, there is a pressing need to enhance not only the tracking algorithms and stabilization mechanisms of UAVs but also to implement advanced signal processing techniques[14].

Considering the issues outlined above, investigations into the development of sophisticated signal processing techniques capable of compensating for these inaccuracies and maintaining the integrity of the vibration data collected become important. While the immediate focus of this research is on

enhancing the reliability and accuracy of structural health assessments for UAV-mounted LDV measurements, the improvements in signal processing methodologies have the potential to be beneficial in a diverse range of applications [11]. These could extend to other remote sensing technologies, vibration analysis in different environments, or even industries where precision measurement under challenging conditions is critical.

2. Time Synchronous Averaging

Time Synchronous Averaging (TSA) is a time-domain based signal processing technique that can be used to extract periodic waveforms in a composite signal. It is commonly used in vibration analysis of rotating machinery by synchronising the signal with the rotational position of the target component such as a gear or bearing [15]. This synchronisation ensures that, at each revolution, the repeating vibration signals from the shaft are constructively added, while non-synchronous noise tends to cancel out through the averaging process. One of the prerequisites for TSA is a reference signal, often acquired from a tachometer or encoder which represents the rotational position or speed of the component being monitored [16].

TSA is particularly advantageous in conditions where the signal-to-noise ratio is low. For instance, when examining the behaviour of a specific gear mesh within a complex gearbox system, the vibrations resulting from the mesh may be overwhelmed by other machine vibrations or ambient noise. In utilising TSA, these gear mesh vibrations can be emphasised such that it becomes possible to detect minute changes in the mesh behaviour that might indicate wear, misalignment, or other faults. By analysing the time-synchronous averaged signal, specialists can infer not only the presence of a fault but in many cases the specific nature and location of that fault within the machinery[17].

CSLDVs output vibration signals that are inherently periodic as they are driven by the operation of motor-controlled mirrors. Time Synchronous Averaging (TSA) presents as a potential signal processing technique for transient noise sources such as drone noise or signal dropouts in CSLDV measurements. When the vibration signals of the LDV is synchronised to the rotation of these mirrors, TSA allows for the precise isolation and analysis of these periodic components from the target vibration amidst potential noise. The goal of using TSA in this scenario is to average out transient sources of noise from the drone and signal loss.

Given a periodic vibration signal, $x(\mathrm{t})$, and noise signal, $w(\mathrm{t})$, we can equate a measurement signal, $y(t)$ containing both a periodic signal (of N cycles) of interest and noise signal by:

$$y(t) = x(t) + w(t), t \in (0, NT] \tag{1}$$

Thus, a TSA of the measurement signal, y_{TSA} can be expressed:

$$y_{TSA} = \frac{1}{N}\sum_{n=0}^{N-1} y(t + nT) \tag{2}$$

$$y_{TSA} = x(t) + \frac{1}{N}\sum_{n=0}^{N-1} w(t + nT), t \in (0, T] \tag{3}$$

In the TSA process, as the number of cycles (N) increases, the noise signal gets progressively averaged towards zero, leading to an enhanced signal-to-noise ratio in the resultant data. However, it's important to note that while TSA effectively suppresses the noise, it also compresses the duration of the signal, resulting in a TSA signal that represents only a single cycle of the periodic waveform. This compression has significant implications for subsequent analysis, particularly when performing Fourier Transformations for frequency domain analysis. The shortened signal duration means that the resultant spectrum from a Fast Fourier Transform (FFT) will have a reduced frequency resolution.

Time Synchronous Moving Average

TSA is known for efficiently suppressing noise and isolating periodic signals, although it has drawbacks in reducing the signal duration – which affects the frequency resolution in subsequent Fourier Transforms. Conversely, moving averaging (MA) preserves signal periodicity and reduces noise, it filters out vital high-frequency signal components. Addressing these issues, Zhang and Hu (2019) introduced the Time-Synchronous Moving Average (TSMA) an enhanced version of TSA that incorporates elements of MA to improve periodic signal detection. TSMA, as proposed by Zhang and Hu, averages the signal over *M* neighboring cycles of the measurement signal. This process acts as an averaging window that moves from the beginning to the end of the original signal, *N*-*M*+1 cycles of the averaged signal can be obtained rather than only 1 cycle as per the TSA. Using the same notation as the TSA with a measurement signal given by eq. (1), the TSMA can be expressed:

$$y_{TMSA} = \frac{1}{M}\sum_{m=0}^{M-1} y(t + mT) \tag{4}$$

$$y_{TMSA} = x(t) + \frac{1}{M}\sum_{m=0}^{M-1} w(t\ +\ mT\ ), \qquad t\ \in\ (0, (N\ -\ M\ +\ 1)T\ ] \tag{5}$$

Multi-cycle Time Synchronous Averaging (TSMA)

Building on the strengths and addressing the limitations of TSA and MA, this paper introduces Multi-Cycle Time-Synchronous Averaging (MCTSA), an alternative technique designed to optimize noise suppression while preserving signal periodicity and high-frequency content. Just like TSA, MCTSA aligns the data with the rotational position of the machinery component, ensuring that periodic signals are constructively combined. However, instead of averaging over the entire signal, MCTSA divides the signal into segments, each consisting of p cycles. Within each segment, the signal is averaged, resulting in a set of N/p averaged segments. These averaged segments are then combined to form the final MCTSA signal:

$$y_{MCTSA}\ (t) = x(t) + \frac{1}{N/p}\sum_{s=1}^{\frac{N}{p}}\left[\sum_{n=(s-1)p}^{sp\ -1} w(t + nT)\right], \qquad t\ \in\ [0, pT\ ) \tag{6}$$

By dividing the signal into segments of p cycles, the method introduces a trade-off between signal length and noise suppression. The final MCTSA signal length is equal to the segment length of p cycles, with longer segments resulting in an extended signal duration (compared to single cycle TSA) but at the expense of noise suppression.

3. Simulating UAV noise and Signal Dropout in CSLDV measurement

Experimental Setup

A CSLDV measurement was conducted on an aluminium rectangular hollow section with length 1m. Its lower end was clamped securely with two clamps, the clamped end was 25 cm, the free end of the beam had a remaining length of 75 cm as shown in figure 1a. The cantilever beam was excited with a small electro-dynamic shaker with an integrated amplifier (K2004E01) which was run using a GW Instek multi-channel function generator (MGF-2260MFA). The output signal from the function generator was recorded on a Siemens Digital Industries Simcenter SCADAS Mobile data acquisition system. The tube was excited near the base of the clamped end, parallel to its smaller dimension. The shaker and cantilever beam were placed on a passive anti-vibration table to minimise ambient vibration thereby ensuring that the measurement reflects the true response of the beam with minimal interference from environmental noise.

A Polytec NLV-2500 Laser Vibrometer was fixed to a bespoke Scanning Laser Doppler Vibrometry Assembly containing a pair of orthogonal motor-controlled mirrors. The LDV output and motor-control inputs were recorded and driven by the SCADAS system. The LDV assembly was placed 1.90 m from the centre of the cantilever beam; the stand-off distance (for visibility maxima) being 2.25m. The tracking filter was set to 'fast' with high and low pass filters turned off. The sensitivity was set to 1000 mm/s/V. The SCADAS mobile device was operated on a laptop using the Simcentre Testlab software running the Spectral Testing application as displayed in figure 1b.

The first resonant frequency of the cantilever beam was estimated to be 17.5 Hz using an analytical approach. During pre-testing a resonance search was conducted around the first resonant frequency, it was found that 17.45 Hz produced the maximum system response, the resonant frequency of the system were updated accordingly. The beam was scanned at 0.25x, 0.5x, 1x and 2x multiples of the beam fundamental frequency ensuring a periodic signal for each scanning cycle; these were 4.363 Hz, 8.725 Hz, 17.45 Hz 34.9 Hz. The SCADAS system was set at a sampling frequency of 102.4 kHz with a measurement window of 30 seconds consisting of 3.072×10^6 samples.

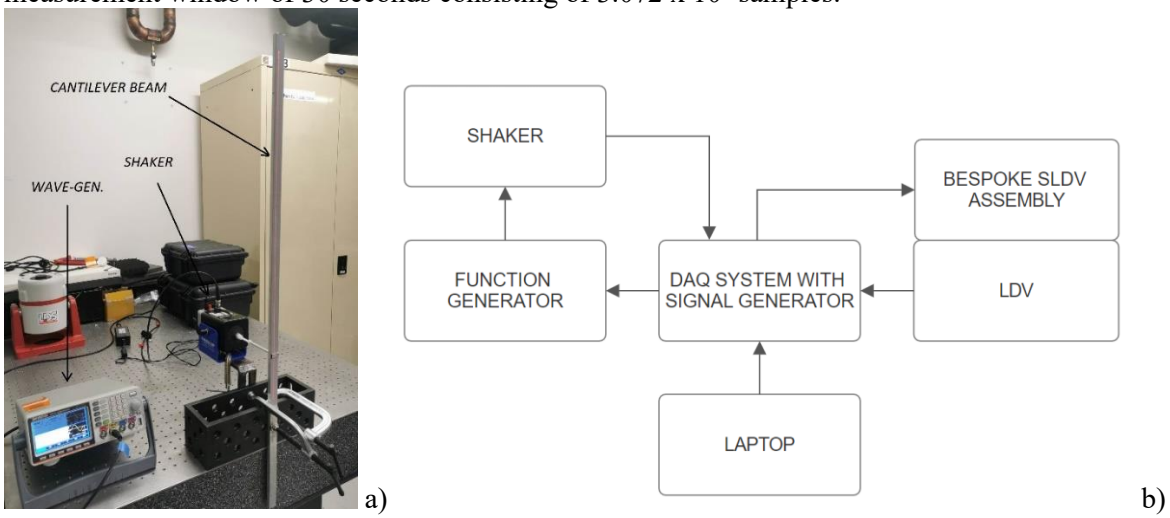

a) b)

Figure 1 – Experimental layout of continuous scanning of cantilever beam; a) actual arrangement, b) block diagram

UAV platform vibration simulation

The DJI Matrice Pro drone is frequently used for high-resolution video/photo capture and presents opportunities for remote LDV measurements. Ge et al. [18] conducted a study that characterised the vibration dynamics of this drone model during flight in the form of a PSD spectra and G_{rms} values.

Using the findings of the study, we simulated the drone's vibration profile by beginning with a linear interpolation of the PSD values across the defined frequency range. An exponential decay was applied to frequencies beyond the highest specified value to simulate the natural decrease in vibration intensity at higher frequencies. Additionally, random phase information was incorporated to create a realistic frequency-domain representation of the noise. Through an inverse Fourier transform, this frequency-domain drone noise profile was converted back into the time domain. This signal encapsulated the intricate vibration patterns of the UAV and was subsequently added to the original LDV signal. The resulting LDV signal carried the characteristics of both the structural vibrations from the CSLDV experiment and the drone-induced vibration providing a realistic representation of the measurement signal expected from UAV-mounted CSLDV campaigns.

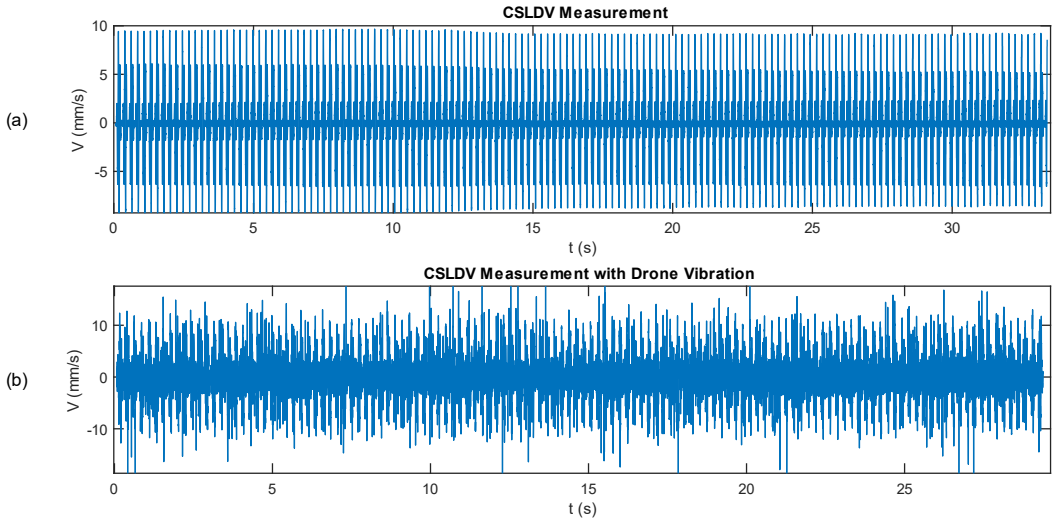

Figure 2: CSLDV signal; a) measured signal, b) simulated signal with drone vibration

Signal dropout simulation

Drones equipped with LDVs must rely on precise tracking systems to maintain focus on the target surface, factors such as drone dynamics and environmental conditions can lead to 'signal dropout,' which results in a loss of signal during measurements. The exact nature, duration and frequency of these signal dropouts depends on multiple factors that vary depending on environmental conditions. As such there is no set manner to replicate signal dropouts. To mimic signal dropouts in LDV-equipped drones, a square wave model was used with 'high' segments representing clear signal collection and 'low' segments for dropouts. An exponential distribution was chosen to model the dropouts to ensure the simulation captures the unpredictable nature of signal dropouts in real world environments, the square wave was randomised with the exponential distribution with the signal dropout rate and average duration of dropouts arbitrarily determined. The parameters used to simulate the dropouts are presented in the table below.

Signal Dropout rate	50%
Average duration of Dropout	1 second
Dropout Distribution	Exponential

Table 1: Signal dropout parameters

Once the square wave with embedded dropouts is prepared, it is multiplied with the CSLDV signal. The resultant signal incorporates the simulated signal dropouts as would be expected from CSLDV measurements from UAVs with frequent signal dropouts.

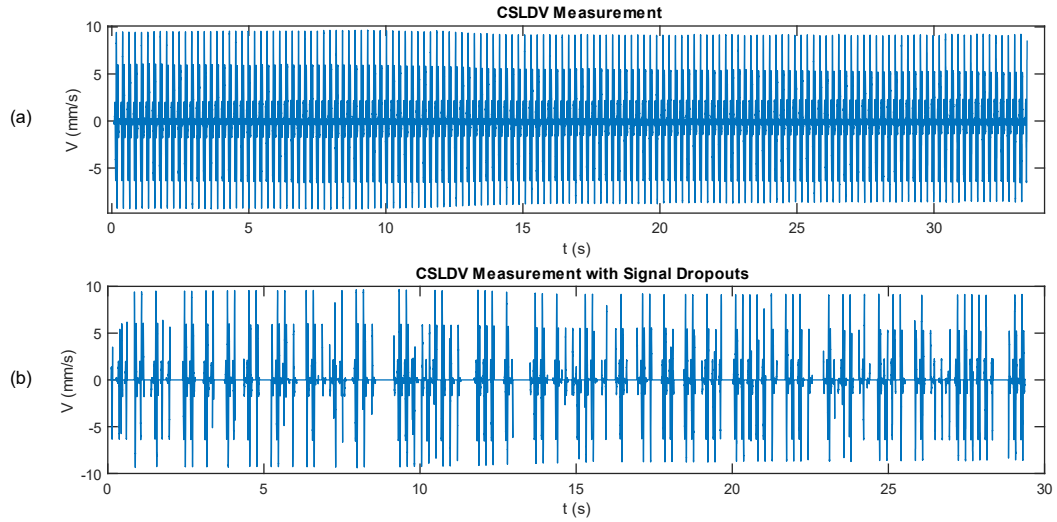

Figure 3: CSLDV signal; a) measured signal, b) simulated signal with dropouts

4. Results

Quantifying signal correction

To critically assess the signal correction efficiency of Time Synchronous Averaging in CSLDV measurements influenced by drone noise and signal dropout, it's vital to establish an appropriate set of evaluation metrics. We achieve this through a two-step process, the initial step calculates the Mean Square Error (MSE) of all the simulated drone dropout/noise signals both before and after TSA. The second step utilises a *R* function with a base-10 logarithm to determine relative changes MSE values pre and post TSA.

Mean Square Error calculation

The Mean Squared Error, or MSE, is a statistical metric commonly used to measure the difference between predicted and observed values. In the context of our research, the MSE is employed to quantify the deviation of the simulated CSLDV signals with drone noise or signal dropout, from our measured CSLDV signal. Our measured CSLDV signal serves as the reference signal, as it was performed in a controlled environment with minimal ambient noise under perfect signal conditions. By analysing the MSE of all the simulated signals, we can determine the baseline signal quality from the reference. We define the MSE of a given signal to be:

$$MSE_{Signal} = \frac{1}{n}\left(\sum_{i=1}^{n}\left(y_{i,\mathrm{sig}} - y_{i,\mathrm{ref}}\right)^2\right) \quad (7)$$

In this expression, n is the total number of data points, $y_{i,\mathrm{sig}}$ is the amplitude of the signal of interest and $y_{i,\mathrm{ref}}$ is the amplitude of the reference CSLDV signal.

R Value calculation

After the MSE of all the signals is calculated we can determine the improvements in signal quality following the TSA using an *R*-value. *R* can be quantified using the mean error reduction of a TSA technique of interest relative to the simulated signal without TSA, given by[10]:

$$R = -10log_{10}\left(\frac{MSE_{Sigal\ with\ TSA}}{MSE_{Signal}}\right) \quad (8)$$

In this expression, $MSE_{Sigal\ with\ TSA}$ is the mean squared error of the noise-affected signal post-TSA application, while MSE_{Signal} is the simulated signal without TSA.

Improvements in CSLDV measurements in the Time-Domain

The figure below illustrates all three TSA techniques on CSLDV measurements experiencing drone noise or signal dropout. In the TSMA an averaging window of three cycles was used and in the MCTSA a segment window of five cycles was used.

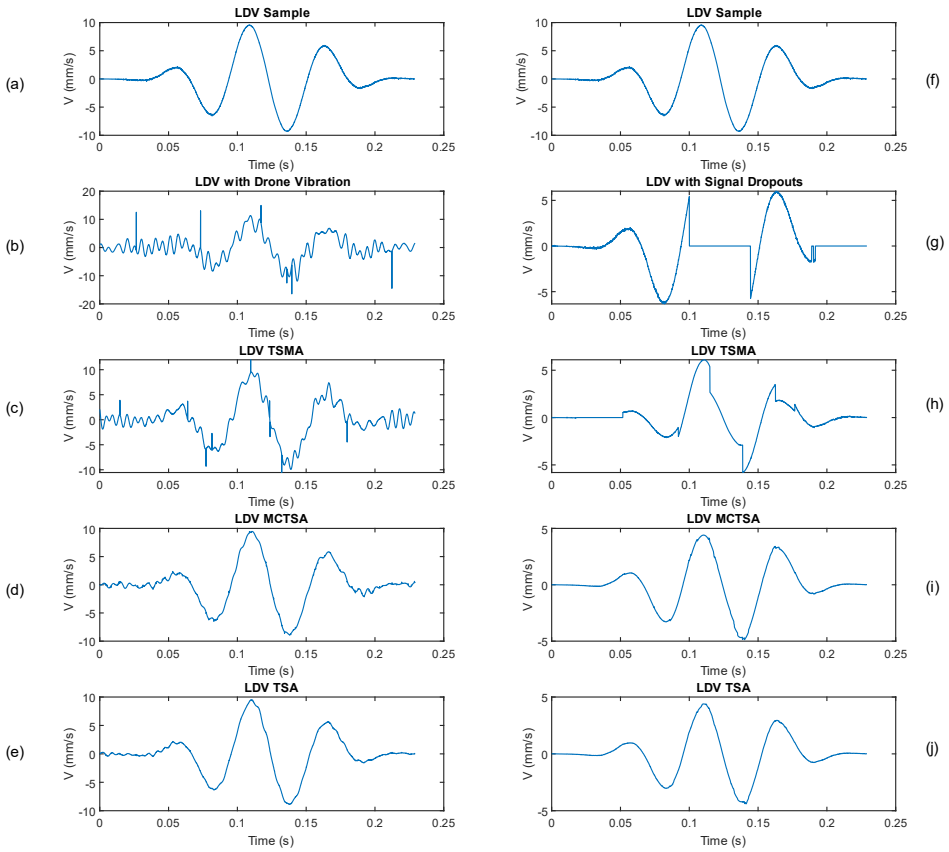

Figure 4: CSLDV signals - Single cycle comparison; a) measured signal, b) simulated signal with drone vibration, c) TSMA of simulated signal with drone vibration, d) MCTSA of simulated signal with drone vibration, e) TSA of simulated signal with drone vibration, f) measured signal, g) simulated signal with dropouts, h) TSMA of simulated signal with dropouts, i) MCTSA of simulated signal with dropouts, j) TSA of simulated signal with dropouts

While all the plots display just a single cycle for clarity, it's important to emphasize that only the TSA signals (e, j) consisted of a single cycle. The improvements in signal quality from the TSA techniques are demonstrated in the below table using the R value described earlier.

	TSA (dB)	**TSMA (dB)**	**MCTSA (dB)**
Drone Vibration	*+8.07*	*+4.27*	*+7.91*
Signal Dropouts	*+3.35*	*+3.02*	*+3.89*

Table 2: R values for all time synchronous techniques

All three TSA techniqiues demonstrate marked improvemennts in suppressing noise from the UAV. The TSA technique yielded the most significant improvement of +8.07 dB, which, when translated via the R metric equautes to a sixfold enhancement in signal quality. Additionally, while all three TSA techniques enhances the signal posed by signal dropout, the extent of improvement is somewhat milder.

Time Synchronous averaging effects in the frequency domain

While the enhancements observed in the time domain are vital to comprehending the efficacy of Time Synchronous Averaging (TSA), understanding its implications in the frequency domain is equally vital. In this regard, a Fast Fourier Transform (FFT) was executed on all the LDV signals to extract both the magnitude and phase of the signals. This allowed for a precise comparison of the changes introduced by the TSA techniques. Presented here are two sets of plots. The first set focuses on the LDV signals influenced by drone vibration, offering a clear visual depiction of the before-and-after effects of the TSA application. The second set provides insights into the LDV signals affected by signal dropouts. Both sets of plots showcase not only the magnitude spectrum but also the phase responses, painting a holistic view of the impact of TSA in the frequency domain.

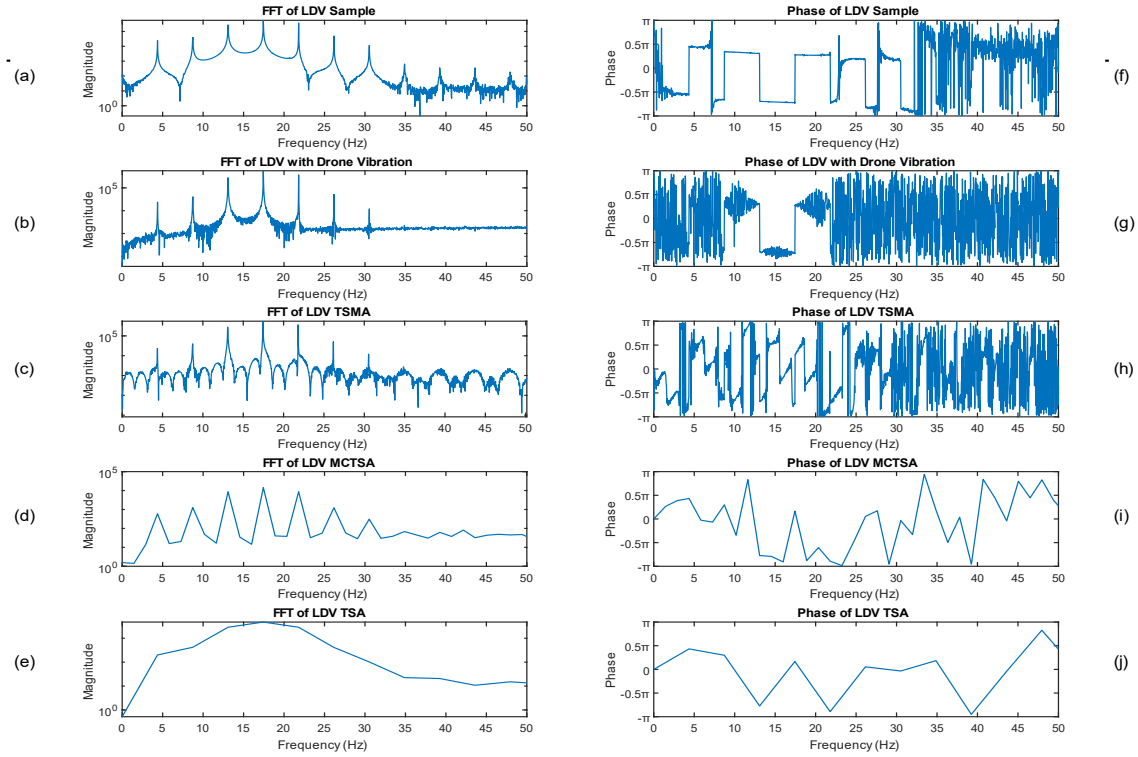

Figure 5: FFT plots; a) magnitude measured signal, b) magnitude simulated signal with drone vibration, c) magnitude TSMA of simulated signal with drone vibration, d) magnitude MCTSA of simulated signal with drone vibration, e) magnitude TSA of simulated signal with drone vibration, f) phase measured signal, g) phase simulated signal with drone vibration, h) phase TSMA of simulated signal with drone vibration, i) phase MCTSA of simulated signal with drone vibration, j) phase TSA of simulated signal with drone vibration

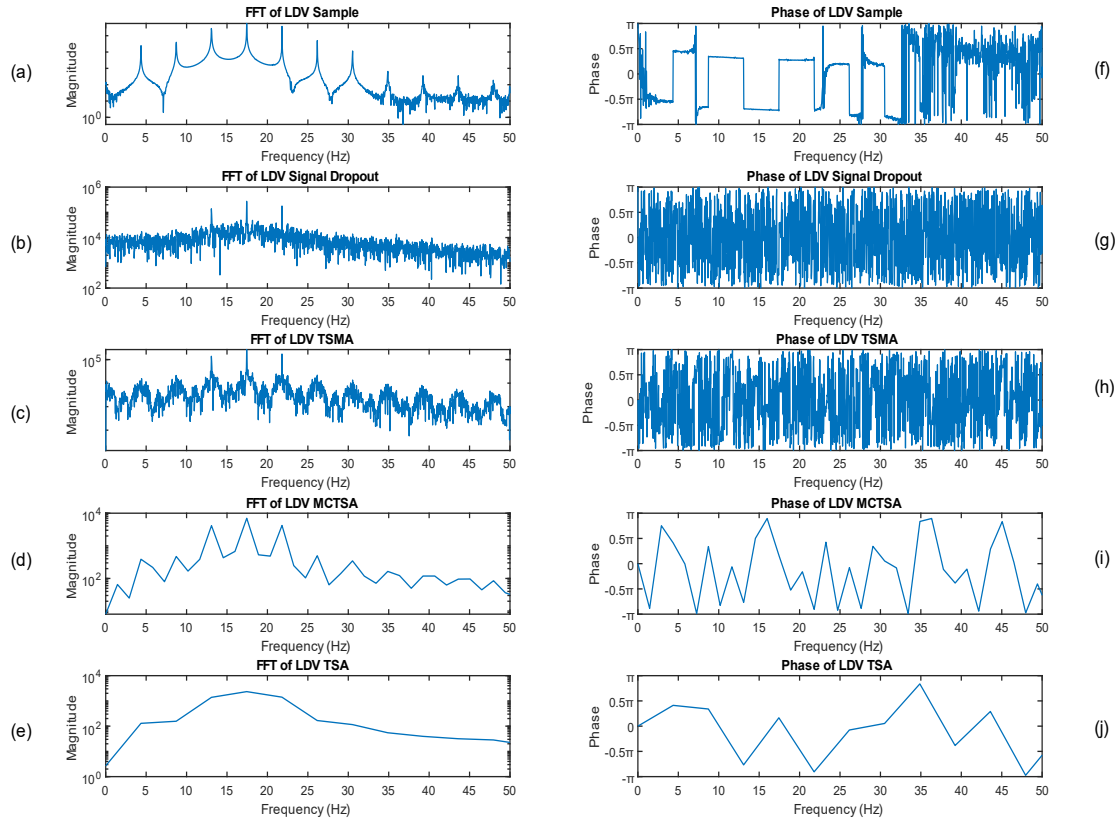

Figure 6: FFT plots; a) magnitude measured signal, b) magnitude simulated signal with dropouts, c) magnitude TSMA of simulated signal with dropouts, d) magnitude MCTSA of simulated signal with dropouts, e) magnitude TSA of simulated signal with dropouts, f) phase measured signal, g) phase simulated signal with dropouts, h) phase TSMA of simulated signal with dropouts, i) phase MCTSA of simulated signal with dropouts, j) phase TSA of simulated signal with dropouts

Following the FFT analyses, the plots reveal important insights into the behaviour of signals in the frequency domain. A primary observation is the loss of phase information in the signal dropout plots, a consequence of the sporadic nature of signal dropouts disrupting consistent phase relationships. The TSA and MCTSA techniques methods introduce a trade-off between signal clarity and signal duration. The reduced signal duration leads to diminished frequency resolution making it difficult to decipher side bands and their relative amplitudes, especially in the TSA.

In contrast to the original and TSMA plots, the TSA and MCTSA frequency responses appear smoother. Specifically, the sidebands and peaks become less pronounced in the TSA plots due to this reduced frequency resolution. The efficacy of TSA in attenuating noise, particularly from drone vibrations, is notable in the lower frequency bands of its spectrum. Concurrently, MCTSA's representation showcases its balance between noise reduction and signal length.

5. Conclusions

This study found that for time-synchronous signal processing techniques to be implemented in CSLDV measurements, it's imperative to sychronise scanning with target vibration, this study implemented time synchronous techniques for CSLDV measurements when target vibration and scanning frequencies were manually synchronised.

Results revealed that all three TSA methods — TSA, TSMA, and MCTSA — significantly mitigate UAV noise and signal dropout. Specifically, TSA and MCTSA techniques demonstrated a notable sixfold enhancement in signal quality when simulated with UAV noise and all three TSA techniques

resulted in a twofold improvement in signal quality when simulated with signal dropouts. These results suggest that TSA techniques may be highly effective when performing CSLDV measurements from UAVs for remote measurements with high levels of drone noise or signal dropouts. However, while TSA and MCTSA bolster signal clarity, they can simultaneously reduce the signal length which subsequently compromises frequency resolution which may be a limiting factor in certain applications.

The necessity for synchronising the scan frequency and target vibration currently prevents the application of TSA in real world measurements where target vibration is unknown. This may be solved by in field algorithms that can estimate target vibration and sychronise scanning accordingly. It's also noteworthy that this investigation was performed in steady-state vibration conditions, underlining the need for further research centered on transient vibration scenarios.

References

1. Rothberg, S., et al., *An international review of laser Doppler vibrometry: Making light work of vibration measurement.* Optics and Lasers in Engineering, 2016. **99**.
2. Halkon, B.J. and S.J. Rothberg, *Towards laser Doppler vibrometry from unmanned aerial vehicles.* Journal of Physics: Conference Series, 2018. **1149**(1): p. 012022.
3. Castellini, P., M. Martarelli, and E.P. Tomasini, *Laser Doppler Vibrometry: Development of advanced solutions answering to technology's needs.* Mechanical Systems and Signal Processing, 2006. **20**(6): p. 1265-1285.
4. Halkon, B. and S. Rothberg, *Vibration measurements using continuous scanning laser vibrometry: Advanced aspects in rotor applications.* Mechanical Systems and Signal Processing, 2006. **20**: p. 1286–1299.
5. Allen, M.S. and M.W. Sracic, *A new method for processing impact excited continuous-scan laser Doppler vibrometer measurements.* Mechanical Systems and Signal Processing, 2010. **24**(3): p. 721-735.
6. Achuthan, K., et al. *A Digital Information Model Framework for UAS-Enabled Bridge Inspection*. Energies, 2021. **14**, DOI: 10.3390/en14196017.
7. Mandirola, M., et al., *Use of UAS for damage inspection and assessment of bridge infrastructures.* International Journal of Disaster Risk Reduction, 2022. **72**: p. 102824.
8. Li, W., et al. *Dynamic Characteristics Monitoring of Large Wind Turbine Blades Based on Target-Free DSST Vision Algorithm and UAV*. Remote Sensing, 2022. **14**, DOI: 10.3390/rs14133113.
9. Halkon, B.J. and S.J. Rothberg, *Reprint of: Taking laser Doppler vibrometry off the tripod: correction of measurements affected by instrument vibration.* Optics and Lasers in Engineering, 2017. **99**: p. 3-10.
10. Darwish, A., et al., *CORRECTION OF LASER DOPPLER VIBROMETER MEASUREMENTS AFFECTED BY SENSOR HEAD VIBRATION USING TIME DOMAIN TECHNIQUES*. 2020. 4842-4850.
11. Mohsan, S.A.H., et al., *Unmanned aerial vehicles (UAVs): practical aspects, applications, open challenges, security issues, and future trends.* Intelligent Service Robotics, 2023. **16**(1): p. 109-137.
12. Darwish, A., B. Halkon, and S. Oberst, *Non-Contact Vibro-Acoustic Object Recognition Using Laser Doppler Vibrometry and Convolutional Neural Networks.* Sensors (Basel), 2022. **22**(23).
13. Daramouskas, I., et al. *Camera-Based Local and Global Target Detection, Tracking, and Localization Techniques for UAVs*. Machines, 2023. **11**, DOI: 10.3390/machines11020315.
14. Lo, L.-Y., et al. *Dynamic Object Tracking on Autonomous UAV System for Surveillance Applications*. Sensors, 2021. **21**, DOI: 10.3390/s21237888.
15. Wang, L., et al., *Time Synchronous Averaging Based on Cross-power Spectrum.* Chinese Journal of Mechanical Engineering, 2023. **36**(1): p. 51.
16. Alimardani, R., A. Rahideh, and S.H. Kia, *Mixed Eccentricity Fault Detection for Induction Motors Based on Time Synchronous Averaging of Vibration Signals.* IEEE Transactions on Industrial Electronics, 2024. **71**(3): p. 3173-3181.
17. Lewis, J.D., *Model-based prediction of otoacoustic emission level, noise level, and signal-to-noise ratio during time-synchronous averaging.* J Acoust Soc Am, 2023. **154**(2): p. 709-720.